

This is a repository copy of *Feasibility and stability in large Lotka Volterra systems with interaction structure*.

White Rose Research Online URL for this paper:

<https://eprints.whiterose.ac.uk/198388/>

Version: Published Version

Article:

Liu, Xiaoyuan, Constable, George William Albert orcid.org/0000-0001-9791-9571 and Pitchford, Jon orcid.org/0000-0002-8756-0902 (2023) Feasibility and stability in large Lotka Volterra systems with interaction structure. *Physical Review E*. 054301. ISSN 1550-2376

<https://doi.org/10.1103/PhysRevE.107.054301>

Reuse



This article is distributed under the terms of the Creative Commons Attribution (CC BY) licence. This licence allows you to distribute, remix, tweak, and build upon the work, even commercially, as long as you credit the authors for the original work. More information and the full terms of the licence here:


<https://creativecommons.org/licenses/>

Takedown

If you consider content in White Rose Research Online to be in breach of UK law, please notify us by emailing eprints@whiterose.ac.uk including the URL of the record and the reason for the withdrawal request.

Feasibility and stability in large Lotka Volterra systems with interaction structure

Xiaoyuan Liu , George W. A. Constable , and Jonathan W. Pitchford
Department of Mathematics, University of York, York, YO10 5DD, United Kingdom

 (Received 24 November 2022; accepted 14 April 2023; published 5 May 2023)

Complex system stability can be studied via linear stability analysis using random matrix theory (RMT) or via feasibility (requiring positive equilibrium abundances). Both approaches highlight the importance of interaction structure. Here we show, analytically and numerically, how RMT and feasibility approaches can be complementary. In generalized Lotka-Volterra (GLV) models with random interaction matrices, feasibility increases when predator-prey interactions increase; increasing competition/mutualism has the opposite effect. These changes have crucial impact on the stability of the GLV model.

DOI: [10.1103/PhysRevE.107.054301](https://doi.org/10.1103/PhysRevE.107.054301)

I. INTRODUCTION

In the 1950s, ecologists such as Odum and MacArthur argued [1,2] that ecosystems with a larger number of species tend to be more stable than less biodiverse systems. This idea was famously mathematized by May in 1972, who applied random matrix theory (RMT) to the problem [3]. May considered perturbations in n species abundances ζ , linearised about a hypothetical fixed point, with near-equilibrium dynamics described by

$$\frac{d\zeta}{dt} = A\zeta, \quad (1)$$

where he suggested parameterising A according to

$$A_{ii} = -1, \quad A_{ij} = \sigma c a_{ij}, \quad (2)$$

with A_{ii} representing the species self-regulation at equilibrium and $a_{ij} \sim \mathcal{N}(0, 1)$ and $c \sim \mathcal{B}(1, C)$. Here A_{ij} represents random species interactions that are nonzero with probability C (referred to as connectance) and when present have standard deviation σ (referred to as interaction strength). Since the asymptotic stability of Eq. (1) is governed solely by its eigenvalues, system-level stability is determined by characterising the eigenvalues of random matrix A .

The eigenvalue distribution of A is uniform across a circle in the complex plane, centered on $(-1, 0)$ and with radius $\sigma\sqrt{nC}$ as $n \rightarrow \infty$ [3–5].

Thus the stability criterion for Eq. (1) is $\sigma\sqrt{nC} < 1$ [see Fig. 1(a)]. This suggests that more diverse ecosystems with more interspecific interactions are less likely to be stable for a given variance in interaction strength.

Allesina and Tang [6] added ecologically-motivated structure to May’s approach, choosing elements of A pairwise by

imposing a correlation ρ between A_{ij} and A_{ji} for $j \neq i$,

$$(A_{ij}, A_{ji}) = \sigma c(a_{ij}, a_{ji}) \quad \text{where} \quad (3)$$

$$(a_{ij}, a_{ji}) \sim \mathcal{N}(\mathbf{0}, \Sigma) \quad \text{with} \quad \Sigma = [(1, \rho), (\rho, 1)],$$

where again $c \sim \mathcal{B}(1, C)$. Ecologically, $\rho < 0$ implies more predator-prey interactions in the ecosystem (A_{ij} and A_{ji} are more likely to have opposite signs), while $\rho > 0$ implies more mutualistic and competitive interactions (A_{ij} and A_{ji} are more likely to have the same sign). Utilizing another RMT result [7,8] they generalized May’s stability criterion to

$$\sigma\sqrt{nC}(1 + \rho) < 1. \quad (4)$$

Thus, increasing the proportion of predator-prey interactions increases stability, whilst increasing the proportion of competitive and mutualistic interactions reduces stability in Eq. (1) [see Fig. 1(a)]. Equation (4) implies that in the extreme limit $\rho \rightarrow -1$, ecosystems are stable as long as there is self-regulation.

These analytic results are independent of the underlying nonlinear model from which they are hypothetically derived. However, this apparent generality conceals an implicit assumption that the fixed point about which the nonlinear system is linearized [to arrive at Eq. (1)] exists and is biologically meaningful. Such biologically meaningful fixed points, where every species is present at a positive abundance, are termed feasible equilibria [9].

We use the generalized Lotka-Volterra model (GLV)

$$\frac{dx}{dt} = x \odot (\mathbf{r} + A\mathbf{x}) \quad (5)$$

to explore the links between the parametrizations of the interaction matrix A in Eqs. (2)–(3) and feasibility. Here x_i is the abundance of species i , r_i is its intrinsic growth rate, A the interaction matrix, and \odot the Hadamard product. Equation (5) has a single nonzero fixed point \mathbf{x}^* , with a Jacobian J , such that

$$\mathbf{x}^* = -A^{-1}\mathbf{r}, \quad J = \text{diag}(\mathbf{x}^*)A. \quad (6)$$

Published by the American Physical Society under the terms of the Creative Commons Attribution 4.0 International license. Further distribution of this work must maintain attribution to the author(s) and the published article’s title, journal citation, and DOI.

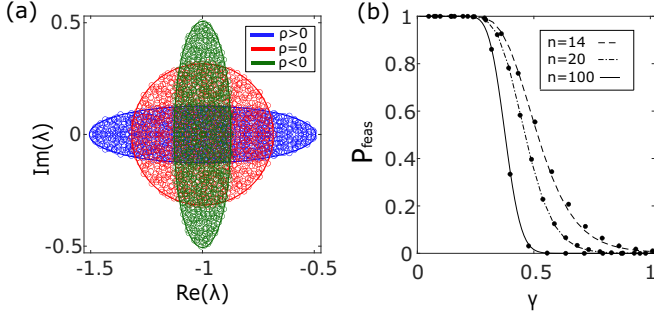


FIG. 1. Panel (a): Eigenvalue distributions of interaction matrix A parameterized according to Eq. (2) (red, $\rho = 0$, see Ref. [3]) and Eq. (3) (blue and green, $\rho \neq 0$, see Ref. [6]), used to infer the stability of the linear model proposed in Eq. (1). Parameter values are $\sigma = 0.01$, $n = 1000$, $C = 1$, and $|\rho| = 0.6$. Panel (b): Feasibility probability P_{feas} , for an ensemble of random fixed points from the nonlinear GLV model, Eq. (5), with interaction matrices parameterized according to Eq. (2) ($\rho = 0$, see Ref. [13]). P_{feas} is plotted as a function of May's complexity parameter $\gamma = \sigma\sqrt{nC}$, for community sizes ranging from $n = 14$ to $n = 100$. In this panel $C = 1$. Curves are analytical predictions and markers are numerical simulations, obtained by sampling 10^4 random interaction matrices A parameterized according to Eq. (2) and calculating the proportion of those that give rise to a feasible equilibrium solution of the GLV model (see Supplemental Material IV [14]).

Note that if the elements of A are drawn from a random distribution, then \mathbf{x}^* is also a random variable (see, for instance, Fig. 2). We denote the multivariate distribution of \mathbf{x}^* as $P(\mathbf{x}^*)$. In particular, there is nothing intrinsic about the structure of \mathbf{x}^* in Eq. (6) that guarantees that it is feasible (i.e., that $x_i^* > 0 \forall i$). Instead, for any given randomly sampled A , there is a probability that the fixed point is feasible, which we denote P_{feas} . The relationships between feasibility, stability, and different system constraints such as interaction structure is a central theme in theoretical ecology [10].

Early analytic insight into the feasibility of \mathbf{x}^* in Eq. (6) assumed that A had interaction coefficients with fixed strengths, or with randomly generated signs [9,11,12]. Stone [13] linked this to May's approach by considering the probability that \mathbf{x}^* is feasible given an ensemble of random interaction matrices

parameterized according to Eq. (2). Under the condition that $r_i = 1 \forall i \in [i, n]$, Stone assumed that such a parametrization of interaction matrices gives rise to a normally distributed x_i^* (see Fig. 2 and Supplemental Material, Sec. VIII [14]).

Stone showed that for a fully connected system $C = 1$, the probability of feasibility is

$$P_{\text{feas}} = 2^{-n} \left(1 + \operatorname{erf} \left(\frac{1}{\gamma_S \sqrt{1 + \gamma_S^2 + \gamma_S^4}} \right) \right)^n, \quad (7)$$

where $\gamma_S = \sigma\sqrt{n}$ is known as the disturbance in Stone's analysis, which is equivalent to May's definition of complexity for the case $C = 1$. We see that P_{feas} drops sharply at a critical value of γ_S , and also has an additional dependence on system size n [see Fig. 1(b)]. By working in the limit $n \rightarrow \infty$, Refs. [15,16] determined a threshold interaction strength above which feasibility is lost in GLV models with interaction matrices parameterized according to Eq. (2). An analytical prediction for the relationship between P_{feas} and the complexity $\gamma = \sigma\sqrt{nC}$ which accounts for C was obtained by Dougoud *et al.* [17]. Akjouj *et al.* [18] investigated the feasibility of sparse ecosystems with interaction matrices that are block structured and d -regular (where each species interacts with d other species). Together these results suggest that feasibility is the more critical measure of complex system stability; compared to linear stability, feasibility is lost at smaller values of complexity.

Here we seek to strengthen the links between RMT [3,19] and feasibility analyses by calculating how the feasibility of an ecosystem changes with complexity [13,17,18,20] when additional species interaction structure is accounted for [6,19]. It was shown by Bunin [10] that feasible systems lose stability above a certain interaction strength by transitioning to a phase with multiple attractors. The interaction strength of this phase transition increases as predator-prey interactions increase. Numerical results by Clenet *et al.* [15] also show that systems biased towards predator-prey interactions lose feasibility at larger interaction strengths than systems without interaction structure, and those biased towards competition and mutualism lose feasibility at smaller interaction strengths than systems without interaction structure. They also obtained

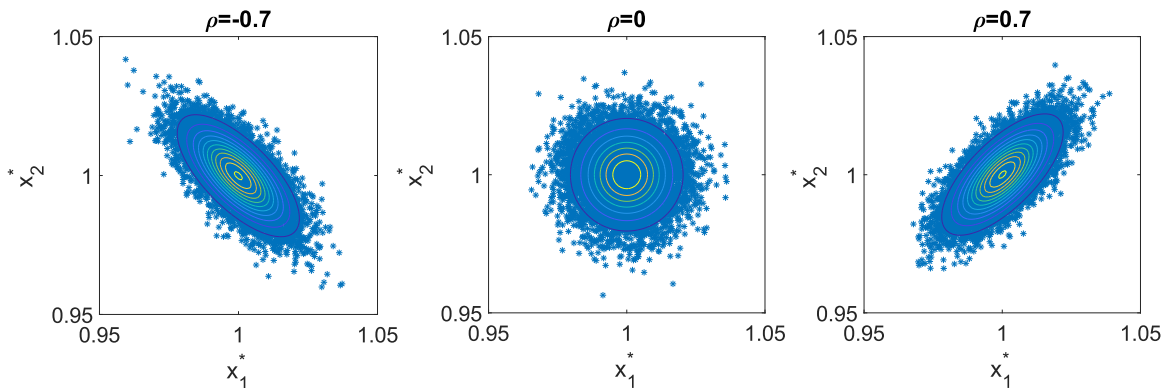


FIG. 2. Plots showing the joint distribution of x_1^* and x_2^* for the GLV model Eq. (5) with $n = 2$, $\sigma = 0.01$, and $C = 1$. Blue markers represent 10^4 numerical solutions of the GLV model, obtained as described in Supplemental Material IV [14]. Contours are analytical predictions for the joint distribution of x_1^* and x_2^* calculated using Eqs. (12)–(14).

an analytical result for the interaction strength above which feasibility is lost, in the limit of large n . In this limit the effect of the correlation parameter ρ , the parameter that governs the proportion of predator-prey or competition/mutualistic interactions, disappears [15]. In this paper, we instead work in the large but finite n limit in order to explore the effect of ρ on the probability of feasibility P_{feas} . In order to calculate P_{feas} , we must also obtain an approximation for the distribution of fixed points. This approximation opens up the possibility of leveraging recent results [21,22] to determine the probability of stability of the GLV model with interaction structure.

II. ANALYSIS

Following Stone [23], we obtain an analytical approximation of $P_{\text{feas}}(\gamma)$ via the distribution of equilibrium species abundances $P(\mathbf{x}^*)$. In particular, Stone [13] applied the Central limit theorem to \mathbf{x}^* in Eq. (9) to argue that $P(\mathbf{x}^*)$ is normal as $n \rightarrow \infty$, and this normality remains a good approximation when n is large but finite (see Supplemental Material, Sec. VIII [14]). The task of calculating the feasibility probability is then equivalent to calculating

$$P_{\text{feas}} = \int_{\mathbf{x}^*=0}^{\infty} P(\mathbf{x}^*) d\mathbf{x}^* \approx \int_{\mathbf{x}^*=0}^{\infty} \mathcal{N}(\boldsymbol{\mu}_{\mathbf{x}^*}, \boldsymbol{\Sigma}_{\mathbf{x}^*}) d\mathbf{x}^*, \quad (8)$$

where $\boldsymbol{\mu}_{\mathbf{x}^*}$ and $\boldsymbol{\Sigma}_{\mathbf{x}^*}$ are respectively the mean and covariance matrix of the species abundances at equilibrium. Note that by symmetry, we can see that for interaction matrices randomly generated according to Eq. (3), $\boldsymbol{\mu}_{\mathbf{x}^*}$ and $\boldsymbol{\Sigma}_{\mathbf{x}^*}$ are themselves highly symmetric, with $[\boldsymbol{\mu}_{\mathbf{x}^*}]_i = [\boldsymbol{\mu}_{\mathbf{x}^*}]_j$, $[\boldsymbol{\Sigma}_{\mathbf{x}^*}]_{ii} = [\boldsymbol{\Sigma}_{\mathbf{x}^*}]_{jj}$, and $[\boldsymbol{\Sigma}_{\mathbf{x}^*}]_{ij} = [\boldsymbol{\Sigma}_{\mathbf{x}^*}]_{ji}$ for all $i, j \in [1, n]$ (i.e., $\boldsymbol{\mu}_{\mathbf{x}^*}$ is a constant vector and the variance-covariance matrix $\boldsymbol{\Sigma}_{\mathbf{x}^*}$ is a double constant matrix [24]).

We now calculate approximations for $\boldsymbol{\mu}_{\mathbf{x}^*}$ and $\boldsymbol{\Sigma}_{\mathbf{x}^*}$. For simplicity we focus on the case $r_i = 1 \forall i$ in Eq. (5). Recall that following Ref. [19], the elements of the interaction matrix A_{ij} and A_{ji} have correlation ρ . Writing $A = \sigma \mathcal{E} - \mathbf{I}$, our fixed point in Eq. (6) can be expressed as a Neumann series [25] for $\|\sigma \mathcal{E}\| < 1$:

$$\mathbf{x}^* = (\mathbf{I} - \sigma \mathcal{E})^{-1} \mathbf{r} \equiv \left(\sum_{j=0}^{\infty} (\sigma \mathcal{E})^j \right) \mathbf{r}. \quad (9)$$

This enables us, in principle, to calculate x_i^* up to an arbitrary order in σ . In our work, we approximate $E(x_i^*)$, $\text{Var}(x_i^*)$, and $\text{Cov}(x_i^*, x_j^*)$ taking into account ρ and C . Using Eq. (9), we approximate $E(x_i^*)$ and $\text{Var}(x_i^*)$ up to and including order σ^6 . Using the fact that the product of an odd number of normal random variables with zero mean have zero expectation, we know that all terms of $E(x_i^*)$ at odd orders of σ vanish. From Eq. (9), we find that the expression for x_i^* at this given order is

$$E(x_i^*) = E \left(1 + \sigma^2 \sum_{\substack{j=1 \\ j \neq i}}^n \sum_{\substack{k=1 \\ k \neq j}}^n \kappa a_{ij} a_{jk} \right) + e_4 \sigma^4 + e_6 \sigma^6, \quad (10)$$

where e_4 and e_6 are coefficients of σ^4 and σ^6 , respectively, in the expectation of x_i^* , and

$$\kappa = \begin{cases} C & \text{if } i = k, \\ C^2 & \text{if } i \neq k, \end{cases} \quad (11)$$

since $i = k$ corresponds to the case where $a_{jk} = a_{ji}$, which corresponds to the case where A_{ij} and A_{ji} are both nonzero with probability C (see Eq. (3) and Allesina and Tang [19]). We use Eq. (10) to illustrate how we obtain our approximation of $E(x_i^*)$. Since $E(a_{ij} a_{ji}) = \rho$, $E(a_{ij}) = 0$, and $E(a_{ij} a_{jk}) = 0$ if $k \neq i$, Eq. (10) is equal to

$$E(x_i^*) = 1 + (n-1)\rho C \sigma^2 + e_4 \sigma^4 + e_6 \sigma^6, \quad (12)$$

where through direct calculation, it can be shown that $e_4 = (n-1)(C + \rho^2(2C + 2C^2(n-2)))$, given by Eq. (S12). Similarly we can calculate e_6 , which is given by Eq. (S53) of the Supplemental Material [14].

An analogous approach can be used to obtain an approximation for $\text{Var}(x_i^*)$ and $\text{Cov}(x_i^*, x_j^*)$ (see Supplemental Material, Sec. I), with $\text{Var}(x_i^*)$ given by

$$\text{Var}(x_i^*) = (n-1)C \sigma^2 + v_4 \sigma^4 + v_6 \sigma^6 + O(\sigma^8), \quad (13)$$

where v_4 and v_6 are the coefficients of σ^4 and σ^6 , respectively, which depend on n , ρ , and C . Specifically, v_4 is the coefficient of σ^4 in Eq. (S20) and v_6 is given by Eq. (S60) in the Supplemental Material [14]. The formulas for v_4 and v_6 are too lengthy to produce here, however of particular note is the fact that they, along with coefficients e_4 and e_6 , are nontrivial polynomials that do not preserve the simple dependence on the complexity parameter γ observed in Refs. [3] or [6]. $\text{Cov}(x_i^*, x_j^*)$ is given by

$$\text{Cov}(x_i^*, x_j^*) = \rho C \sigma^2 + c_4 \sigma^4 + O(\sigma^6), \quad (14)$$

where $c_4 = (3 + (6 + C(5n - 11))\rho^2)$. While we could extend this approximation to order σ^6 , we note that this makes little quantitative difference to the approximation. In the expression for $\text{Cov}(x_i^*, x_j^*)$, the coefficient of each order of σ is a factor of n smaller than the corresponding coefficients in the expression for $E(x_i^*)$ and $\text{Var}(x_i^*)$ (see Supplemental Material, Sec. VII [14]). This implies that for a fixed value of large but finite n , $\text{Cov}(x_i^*, x_j^*)$ increases more slowly with σ than $E(x_i^*)$ and $\text{Var}(x_i^*)$, and thus $\text{Cov}(x_i^*, x_j^*)$ plays a smaller role in governing how $P(\mathbf{x}^*)$, and similarly P_{feas} , varies with σ . It is therefore possible to approximate $\text{Cov}(x_i^*, x_j^*)$ to order σ^4 without sacrificing the accuracy of the analytical prediction of P_{feas} . The slower increase in $\text{Cov}(x_i^*, x_j^*)$ with σ is verified numerically in Fig. S7. Since an analytical approximation of $\text{Cov}(x_i^*, x_j^*)$ to order σ^6 requires considerably more algebra (see Supplemental Material, Sec. ID5 [14]) without conferring significant improvements to the accuracy of P_{feas} , we restrict our analysis to the order σ^4 approximation given in Eq. (14).

Equations (12)–(14) are then used to construct $\boldsymbol{\mu}_{\mathbf{x}^*}$ and $\boldsymbol{\Sigma}_{\mathbf{x}^*}$ in Eq. (8). Note that we expect our approximation to hold when n is large [such that $P(\mathbf{x}^*)$ is approximately normal, see Eq. (8)] and when σ is small [such that the expansions in Eqs. (12)–(14) remain sufficient]. When these conditions are not met, the approximations given in Eqs. (12)–(14) break down at lower values of $|\rho|$. For instance in a 25 species ($n = 25$) system, the analytical approximation of $\text{Var}(x_i^*)$ in Eq. (13) loses accuracy when $|\rho| > 0.25$, while for a 100 species system $\text{Var}(x_i^*)$ remains accurate up to $|\rho| = 0.5$ (see Supplemental Material, Sec. II [14]).

The fact that our normal distributions feature such a high degree of symmetry, with $\boldsymbol{\mu}_{\mathbf{x}^*}$ a constant vector and $\boldsymbol{\Sigma}_{\mathbf{x}^*}$

a double constant matrix, allows us to further simplify the calculation of P_{feas} . This provides ease of computation for large systems. Using the results of Ref. [26], which expresses integrals over the cubic region of the variable space, Eq. (8) can be reduced to an expression involving a single integral, given by

$$P_{\text{feas}} = \int_{-\infty}^{\infty} \left\{ \prod_{i=1}^n \Phi \left(\frac{y_i - b_i u}{(1 - b_i^2)^{1/2}} \right) \right\} \phi(u) du, \quad (15)$$

where $\phi(u)$ is the density function of a standard normal random variable u and $\Phi(v)$ denotes the cumulative distribution function of a standard normal random variable v . In our analytical prediction of P_{feas} , we have that $y_i = \frac{E(x_i^*)}{\sqrt{\text{Var}(x_i^*)}}$ and

$b_i = \frac{\sqrt{\text{Cov}(x_i^*, x_j^*)}}{\text{Var}(x_i^*)}$ (see Supplemental Material, Sec. III [14]). In other words, P_{feas} is the expression obtained by substituting these expressions for y_i and b_i into Eq. (15). (see Supplemental Material, Sec. III). Interestingly, note that in the results of Refs. [3,19], C appears as a compound parameter with σ^2 , but in Eqs. (12)–(14), C appears in a complicated polynomial form. The analytical prediction of $P_{\text{feas}}(\gamma)$ is shown in Figs. 3 (a)–(b). Moreover, the fact that $\text{Cov}(x_i^*, x_j^*)$ is a factor of n smaller than $\text{Var}(x_i^*)$ partly explains the observation of Clenet [15] that as $n \rightarrow \infty$, the effect of ρ on P_{feas} completely disappears.

III. RESULTS

A. Predator-prey interactions increase the feasibility of random ecosystems

The qualitative difference in how P_{feas} changes with the complexity γ as the correlation ρ is varied is shown analytically in Fig. 3. For a given value of n , when ρ is positive (blue), feasibility is lost at a smaller complexity compared to the case where $\rho = 0$ (red). However when ρ is negative (green), we observe the opposite effect whereby feasibility is lost at a larger complexity than the case $\rho = 0$.

It can be seen in Fig. 3 that the magnitude of the difference between $P_{\text{feas}}(\gamma, \rho)$ and $P_{\text{feas}}(\gamma, 0)$ also varies with γ . For instance when γ is sufficiently small, there is no difference between $P_{\text{feas}}(\gamma, \rho)$ and $P_{\text{feas}}(\gamma, 0)$, since P_{feas} is 1 regardless of ρ . The bottom panels of Fig. 3 below plot this difference, demonstrating how it varies with γ . The difference between $P_{\text{feas}}(\gamma, \rho)$ and $P_{\text{feas}}(\gamma, 0)$ is the greatest for intermediate values of complexity γ , where the system is transitioning rapidly away from feasibility. For a given system size n , the magnitude of this difference ($|P_{\text{feas}}(\gamma, \rho) - P_{\text{feas}}(\gamma, 0)|$) also increases with the magnitude of ρ .

In Supplemental Material IE [14], we see that for all values of ρ , the loss of feasibility in the GLV model with Allesina and Tang type interaction matrices occurs at a smaller complexity than the loss of stability in the corresponding linear model. As an extreme example, in linear systems comprising all predator-prey interactions ($\rho = -1$) stability is guaranteed regardless of ecosystem complexity [see Eq. (4)]; conversely, feasibility is still lost above a critical value of the complexity parameter γ (see Fig. S2 of Supplemental Material [14]). Figure 3 demonstrates that the analytical results in Eqs. (12)–(14) can be used to accurately predict P_{feas} as a function

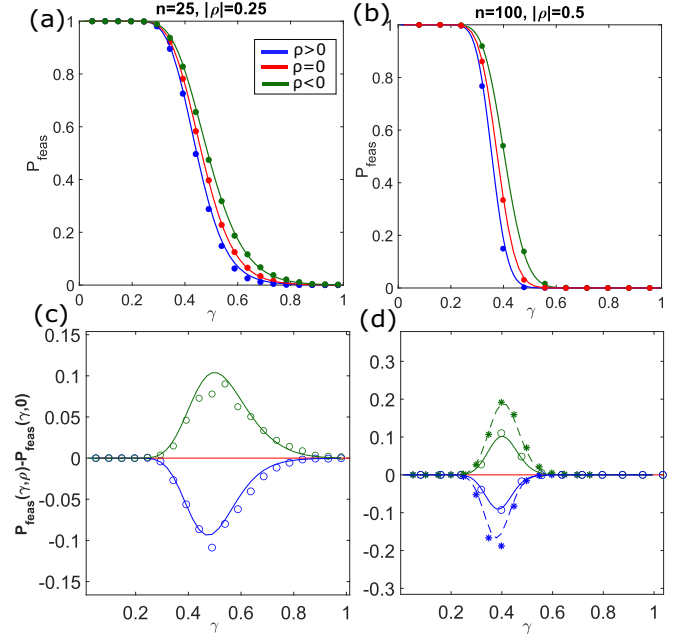


FIG. 3. Panels (a) and (b) plot the feasibility probability P_{feas} as a function of complexity γ for systems with ecologically motivated interaction structure: Blue ($\rho > 0$) biased toward competitive/mutualistic interactions; red ($\rho = 0$) unbiased interactions; green ($\rho < 0$) biased towards predator-prey interactions. Panels (c) and (d) plot the difference between P_{feas} in systems with $\rho \neq 0$ and P_{feas} in systems where $\rho = 0$ [$P_{\text{feas}}(\gamma, \rho) - P_{\text{feas}}(\gamma, 0)$] as a function of γ , with lines the prediction derived from Eq. (15) and markers the results of numerical simulation. In panel (c), $n = 25$ and hollow circles show the results of numerical simulations for the case $|\rho| = 0.25$. In panel (d), where $n = 100$ (and our approximations are valid for larger values of ρ) hollow circles again represent the case $|\rho| = 0.25$, while asterisks are numerical simulations for the case $|\rho| = 0.5$. Numerical simulations are obtained by sampling 10^4 random interaction matrices A parameterized according to Eq. (2) and calculating the proportion of those that give rise to a feasible equilibrium solution of the GLV model Eq. (5) (see Supplemental Material, Sec. IV [14]).

of γ in the case where $C = 1$. Furthermore, Supplemental Material, Sec. V [14] shows that the same analytical results remain highly accurate for predicting P_{feas} as a function of γ in the case where $C = 0.3$. By comparing the feasibility probabilities of such a system with that of a fully connected system, we see that a sparsely connected system of $n = 100$ shows an almost identical feasibility-complexity relation as a fully connected system.

Most importantly, in Eqs. (12)–(14) we have analytically approximated the distributions of x_i^* for nonlinear GLV models Eq. (5) where the underlying interaction matrix A is constructed according to Eq. (3). This opens up the possibility to extend these results to predict the stability of GLV models with ecologically motivated interaction structures. Such a stability analysis is beyond the scope of this work, but would be attainable through detailed analysis of the GLV Jacobian. In the next section we investigate how this might be achieved within the scope of existing methods.

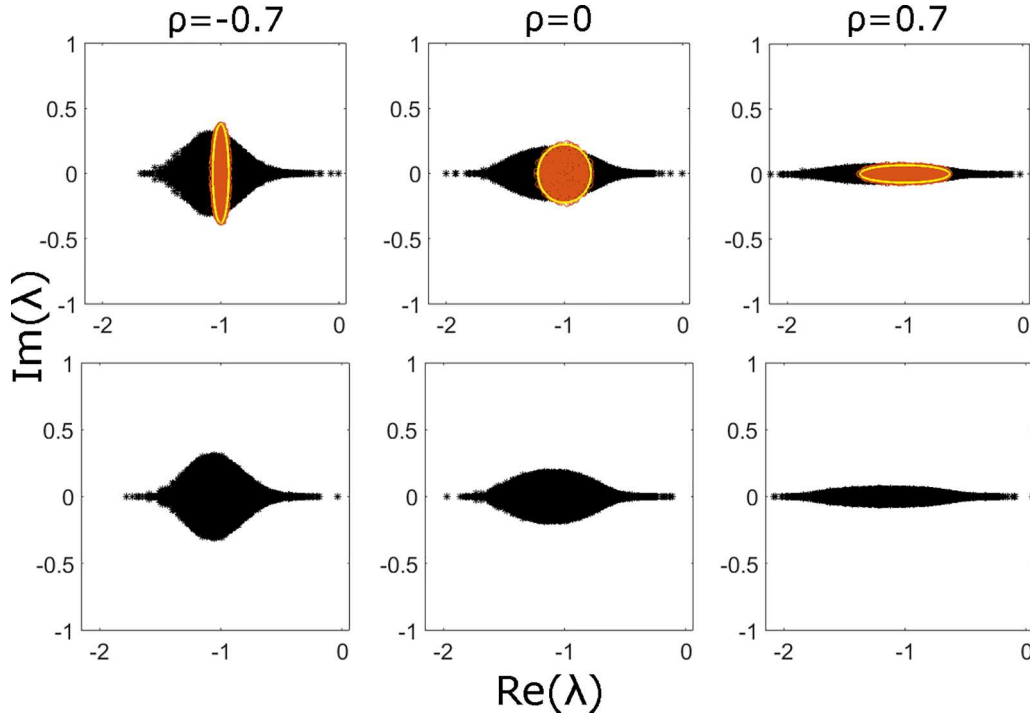


FIG. 4. Top row: Orange ellipses are eigenvalue distributions of A where A is parameterized according to Eqs. (2)–(3). Yellow boundaries are predicted by Allesina and Tang. Black markers represent 50 realisations of the eigenvalue distribution of the GLV Jacobian $J = \mathbf{x}^*A$ where the exact \mathbf{x}^* corresponding to each given A is used. Bottom row: 50 realisations of the eigenvalue distribution of $J = \mathbf{x}^*A$ where elements of \mathbf{x}^* are sampled independently of A , from the multivariate normal distribution characterized by Eqs. (12)–(14). Parameter values are $\sigma = 0.01$, $n = 500$, and $C = 1$. Given these parameters, Eqs. (12)–(14) predict that in the left panel $P_{\text{feas}} = 0.993$, middle panel $P_{\text{feas}} = 0.997$, and right panel $P_{\text{feas}} = 1.000$.

B. Comparing RMT predictions with GLV Jacobian matrices

Gibbs *et al.* [21] studied the eigenvalue distribution of a matrix that is assumed to be of the same structure as the GLV Jacobian [Eq. (6), right], where J is decomposed into a product of an interaction matrix A and fixed points \mathbf{x}^* . However, for simplicity, they assume that the distribution from which \mathbf{x}^* is drawn is independent of A , whereas this is clearly not the case [Eq. (6), left].

Gibbs’ assumption of independence between the random elements of A and \mathbf{x}^* means that cross-correlations between them need not be considered, thereby simplifying the analysis. We test whether this assumption holds, in order to determine whether Gibbs’ method may be applicable to calculating the eigenvalue distribution of the GLV Jacobian [Eq. (6)]. To do so, we first calculate the eigenvalue distribution of $J = \mathbf{x}^*A$ where the elements of \mathbf{x}^* are sampled independently to those of A . The distribution from which we sample the elements of \mathbf{x}^* is a normal distribution with $E(x_i^*)$, $Var(x_i^*)$, and $Cov(x_i^*, x_j^*)$ given by Eqs. (12)–(14), which we approximated. A is constructed according to Eq. (3). We then compare this eigenvalue distribution (shown in Fig. 4, bottom panels) to that of the GLV Jacobian where the exact \mathbf{x}^* corresponding to each given A is used (shown in black markers of Fig. 4, top panels).

By comparing the black markers on the top panels with those of the bottom panels of Fig. 4, we see that our method of sampling \mathbf{x}^* independently of A from our distribution of \mathbf{x}^* works well in predicting the eigenvalue distribution of

the GLV Jacobian. This comparison is conducted in a region where feasibility is almost surely guaranteed. From the top panels, we see that when the correlation parameter is negative, i.e., $\rho < 0$, the bulk eigenvalue distribution of J gets stretched in the $Im(\lambda)$ plane, and when $\rho > 0$ in the $Re(\lambda)$ plane. This qualitative effect is consistent with the result of Allesina and Tang [19]. It is shown numerically in Supplemental Material, Sec. VI [14] that increasing ρ decreases the average resilience of the GLV model.

The average maximum outlier eigenvalue (averaged over multiple realizations of the interaction matrix A) is also correctly predicted by our theory, which relies on the assumption of statistical independence between A and our calculated distribution of \mathbf{x}^* [see Eqs. (12)–(14)], as illustrated in Fig. S6(a). However, our theory does not correctly predict the maximum outlier eigenvalue of individual realizations of the GLV Jacobian. This suggests that cross-correlations between the entries of A and \mathbf{x}^* may be quantitatively important in calculating the stability of individual realizations of the GLV model. As the stability of a system is governed solely by the eigenvalue with the largest real part, a stability analysis of the GLV model must be preceded via calculating such an eigenvalue. Below, we provide an insight into some possible techniques for calculating the stability of the GLV model with Allesina and Tang type interaction matrices.

Stone [20] showed that, provided that $|\sigma \mathcal{E}|$ is sufficiently small, the eigenvalue with the largest real part (outlier eigenvalue of J) is approximately equal to minus the abundance of the least abundant species, i.e., $\lambda_{\text{max}} \approx -\min_{i \in \{1, n\}} x_i^*$; in

which case we have the weak condition whereby feasibility corresponds to the local asymptotic stability of the GLV model. In the case where $\rho = 0$ or $|\rho|$ is small, $-\min_{i \in \{1, n\}} x_i^*$ is an accurate estimate of the outlier eigenvalue of J , however this accuracy breaks down as we increase $|\rho|$ (see Supplemental Material, Sec. VI [14]).

Relying on Gibbs' assumption allows us to accurately capture the bulk eigenvalue distribution of J and the effect that the correlation parameter ρ has on the average resilience over a large number of realisations [see Fig. S6(a)], although it fails to accurately calculate the outlier eigenvalue of J corresponding to a specific realization of A .

IV. DISCUSSION

We have obtained an analytical prediction of the feasibility probability as a function of complexity $\gamma = \sigma\sqrt{nC}$ for random GLV models with interaction matrices of Allesina and Tang type [19]. By extending the analytical result of Ref. [15] to the case of large but finite n , we have shown that a positive value of ρ reduces the feasibility probability for a given complexity, while a negative value of ρ increases the corresponding feasibility probability, an effect not quantifiable in the infinite n limit. We have also accounted for the connectance C . Since natural ecological systems are sparsely connected [27], both these generalizations mentioned above add biological realism to the result of Stone (2016) [23]. Relationships between complexity and feasibility have also been studied by Ref. [28], where they characterized feasibility by how freely one could choose the intrinsic growth rate vectors to allow the system to remain feasible. As a whole, these results strengthen connections between feasibility and RMT systems, whilst also adding biological realism.

Along the way, we managed to analytically approximate the distribution of \mathbf{x}^* as a function of the system parameters n , C , σ , and ρ . In doing so, we emphasize how the small covariance between the abundances of species can partly explain the observation of Ref. [15] that the effect of interaction structure on feasibility completely disappears as $n \rightarrow \infty$. Most importantly, our approximation of the distribution of \mathbf{x}^* has allowed us to check the utility of Gibbs' assumption of independence between \mathbf{x}^* and A in predicting the eigenvalue distribution of the GLV Jacobian for systems with Allesina and Tang type interaction matrices [20,21]. Figure 4 shows that Gibbs' assumption can be used to accurately predict the effect of interaction structure [19] on the eigenvalue distribution of feasible random GLV models. However, relying on this assumption does not allow us to accurately calculate the outlier eigenvalue of the GLV Jacobian for a particular realization.

It is of note that our method for calculating the feasibility probability relies on several assumptions on the parameter values to ensure accuracy (see Supplemental Material, Secs. I E and II [14]). We also assumed that x_i^* is normally distributed. Since the Neumann series approximation for x_i^* is normal in the limit $n \rightarrow \infty$, and is convergent if and only if

$\sigma\sqrt{nC} < 1$, our method is accurate for large n and small σ (see Supplemental Material, Sec. VIII). Since the Neumann series expansion is precise, it is straightforward to extend our analysis to arbitrary orders of precision by working to higher orders in σ [see Eq. (9)].

The concept of feasibility has been associated with the extinction probability. It was summarized by Stone (1988) [13] that a higher feasibility probability is linked to the reduction in the probability of extinction following structural disturbances, which are changes in interaction strengths caused by environmental change. Our results imply that increasing predator-prey interactions reduces the chance of extinction following structural disturbances.

We have used the assumption of May (1972) that all species are self-regulating [3]. This is representative of natural ecosystems since they require 50 percent of species to self-regulate to allow for stability [29]. However, the assumption that $r_i = 1 \forall i \in [1, n]$ may not be biologically realistic, as natural ecosystems contain consumer species which do not grow in isolation. This is an interesting area for future investigation, however it was suggested by Song *et al.* [30] that this assumption gives the parameter region where feasible systems are likely to be present.

Having generalized the distribution of \mathbf{x}^* to account for arbitrary ρ , we have opened up the possibility for extending the results of Gibbs *et al.* [21] to analytically predict the boundary of the eigenvalue distribution of the GLV Jacobian of such systems. This would enable us to calculate the stability of such GLV models. One potential method to perform this calculation is by applying the cavity method as detailed in Ref. [21]. It may also be possible to calculate the expected value of $-\min_{i \in \{1, n\}} x_i^*$ by applying order statistics as detailed in Ref. [31], and thus the expected resilience of a GLV model with a given value of ρ , although this is only applicable to systems where $|\rho|$ is small. We note, also, that the analytical approaches central to this study lead to predictions of normal distributions of steady-state species abundances. Empirical evidence is typically scale dependent and points to a range of more complex possible species-abundance distributions [32] and the development of scale-dependent theory to bridge this gap with models may be a fruitful line of further enquiry.

Overall, our analyses, combined with Refs. [15,19,31], show that increasing the proportion of predator-prey interactions not only increases feasibility, but also the resilience of feasible GLV models. This provides greater support to Allesina and Tang's [19] conclusion that predator-prey interactions are stabilizing whilst competitive/mutualistic interactions are destabilizing.

ACKNOWLEDGMENTS

The Complexity and Stability reading group is an unfunded research grouping at the University of York. The Ph.D. studentship (X.L.) is funded by the University of York through the EPSRC DTP, Grant No. EP/V52010X/1, is greatly acknowledged.

[1] E. P. Odum, Fundamentals of ecology (1953), *The Future of Nature* (Yale University Press, 2013), pp. 233–144.

[2] R. MacArthur, Fluctuations of animal populations and a measure of community stability, *Ecology* **36**, 533 (1955).

- [3] R. M. May, Will a large complex system be stable? *Nature (London)* **238**, 413 (1972).
- [4] E. P. Wigner, On the distribution of the roots of certain symmetric matrices, *Ann. Math.* **67**, 325 (1958).
- [5] T. Tao, V. Vu, and M. Krishnapur, Random matrices: Universality of esds and the circular law, *Ann. Probab.* **38**, 2023 (2010).
- [6] S. Allesina and S. Tang, Stability criteria for complex ecosystems, *Nature (London)* **483**, 205 (2012).
- [7] V. L. Girko, Elliptic law, *Theory Probab. Appl.* **30**, 677 (1986).
- [8] H. J. Sommers, A. Crisanti, H. Sompolinsky, and Y. Stein, Spectrum of Large Random Asymmetric Matrices, *Phys. Rev. Lett.* **60**, 1895 (1988).
- [9] A. Roberts, The stability of a feasible random ecosystem, *Nature (London)* **251**, 607 (1974).
- [10] G. Bunin, Ecological communities with lotka-volterra dynamics, *Phys. Rev. E* **95**, 042414 (2017).
- [11] M. E. Gilpin, Stability of feasible predator-prey systems, *Nature (London)* **254**, 137 (1975).
- [12] B. S. Goh and L. S. Jennings, Feasibility and stability in randomly assembled lotka-volterra models, *Ecol. Modell.* **3**, 63 (1977).
- [13] L. Stone, Some problems of community ecology: Processes, patterns and species persistence in ecosystems, Ph.D. thesis, Monash University, 1988.
- [14] See Supplemental Material at <http://link.aps.org/supplemental/10.1103/PhysRevE.107.054301> for details of analytical expressions and derivations; implementation of numerical simulations; parameter regions where our analytical approximations remain accurate; demonstration of how the assumption of independence between the interaction coefficients and species abundance distribution may accurately predict the resilience of the GLV system.
- [15] M. Clenet, H. El Ferchichi, and J. Najim, Equilibrium in a large lotka-volterra system with pairwise correlated interactions, *Stoch. Process. Their Appl.* **153**, 423 (2022).
- [16] P. Bizeul and J. Najim, Positive solutions for large random linear systems, *Proc. Am. Math. Soc.* **149**, 2333 (2021).
- [17] M. Dougoud, L. Vinckenbosch, R. P. Rohr, L.-F. Bersier, and C. Mazza, The feasibility of equilibria in large ecosystems: A primary but neglected concept in the complexity-stability debate, *PLoS Comput. Biol.* **14**, e1005988 (2018).
- [18] I. Akjouj and J. Najim, Feasibility of sparse large Lotka-Volterra ecosystems, *J. Math. Biol.* **85**, 66 (2022).
- [19] S. Allesina and S. Tang, The stability-complexity relationship at age 40: A random matrix perspective, *Popul. Ecol.* **57**, 63 (2015).
- [20] L. Stone, The feasibility and stability of large complex biological networks: A random matrix approach, *Sci. Rep.* **8**, 8246 (2018).
- [21] T. Gibbs, J. Grilli, T. Rogers, and S. Allesina, Effect of population abundances on the stability of large random ecosystems, *Phys. Rev. E* **98**, 022410 (2018).
- [22] J. W. Baron, T. J. Jewell, C. Ryder, and T. Galla, Eigenvalues of Random Matrices with Generalized Correlations: A Path Integral Approach, *Phys. Rev. Lett.* **128**, 120601 (2022).
- [23] L. Stone, The google matrix controls the stability of structured ecological and biological networks, *Nat. Commun.* **7**, 1 (2016).
- [24] B. O'Neill, The double-constant matrix, centering matrix and equicorrelation matrix: Theory and applications, [arXiv:2109.05814](https://arxiv.org/abs/2109.05814) (2021).
- [25] R. Kress, *Linear Integral Equations* (Springer, New York, 2014).
- [26] R. N. Curnow and C. W. Dunnett, The numerical evaluation of certain multivariate normal integrals, *The Annals of Mathematical Statistics* (JSTOR, 1962), pp. 571–579.
- [27] M. R. Gardner and W. R. Ashby, Connectance of large dynamic (cybernetic) systems: Critical values for stability, *Nature (London)* **228**, 784 (1970).
- [28] J. Grilli, M. Adorasio, S. Suweis, G. Barabás, J. R. Banavar, S. Allesina, and A. Maritan, Feasibility and coexistence of large ecological communities, *Nat. Commun.* **8**, 14389 (2017).
- [29] G. Barabás, M. J. Michalska-Smith, and S. Allesina, Self-regulation and the stability of large ecological networks, *Nat. Ecol. Evol.* **1**, 1870 (2017).
- [30] C. Song and S. Saavedra, Will a small randomly assembled community be feasible and stable? *Ecology* **99**, 743 (2018).
- [31] S. Pettersson, V. M. Savage, and M. N. Jacobi, Predicting collapse of complex ecological systems: Quantifying the stability-complexity continuum, *J. R. Soc., Interface* **17**, 20190391 (2020).
- [32] L. H. Antão, A. E. Magurran, and M. Dornelas, The shape of species abundance distributions across spatial scales, *Front. Ecol. Evol.* **9**, 626730 (2021).